Novel D-Seco Paclitaxel Analogues: Synthesis, Biological Evaluation, and Model Testing

Luciano Barboni,† Apurba Datta, Dinah Dutta, Gunda I. Georg,* and David G. Vander Velde

Department of Medicinal Chemistry and Drug Discovery Program, Higuchi Biosciences Center, University of Kansas, Lawrence, Kansas 66045

Richard H. Himes

Department of Molecular Biosciences, University of Kansas, Lawrence, Kansas 66045

Minmin Wang and James P. Snyder

Department of Chemistry, Emory University, Atlanta, Georgia 30322

georg@ku.edu

Received November 1, 2000

Four new D-secopaclitaxel analogues were synthesized from paclitaxel. The key step of the synthesis involved the opening of the D-ring by Jones oxidation. Two of the compounds had been predicted to be nearly as active as paclitaxel in a minireceptor model of the binding site on tubulin, but all were biologically inactive in an in vitro cytotoxic assay and a tubulin assembly assay. The biological results identify a weakness in our predictive minireceptor model and suggest a corrective remedy in which additional amino acids are needed to accommodate ligand−protein steric effects around the oxetane ring. These changes to the model lead to correct predictions of the bioactivity. Conformational analysis and dynamics simulations of the compounds showed that the 4-acetyl substituent is as important as the oxetane in determining the A ring conformation.

Paclitaxel (**1**), first isolated from the bark of *Taxus brevifolia*,[1] and its semisynthetic analogue docetaxel (**2**),

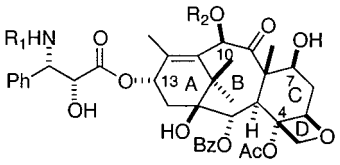

R_1 = Bz, R_2 = Ac, Paclitaxel (**1**)
R_1 = Boc, R_2 = H, Docetaxel (**2**)

obtained from 10-deacetylbaccatin III, are important therapeutic agents clinically used for the treatment of a variety of cancers.[2−5] Their mechanism of action involves disruption of microtubule dynamics, thereby blocking cell division.[6] Recently, other structurally diverse products, epothilones A and B, eleutherobin, and discodermolide, have been found to have the same mechanism of action.[7] They are believed to share the same or overlapping binding sites because they are competitive inhibitors of [^{3}H]paclitaxel binding to microtubules.[7] Clearly, the complete understanding of the minimal structural requirements to maintain microtubule binding and the identification of a three-dimensional pharmacophore common to these drugs are essential for the development of new compounds with increased biological activity. SAR studies on paclitaxel have been extensive and have led to the conclusion that the C13 side chain and the ester groups at C2 and C4 are essential for biological activity.[8] A remarkable exception is the recent report that a taxane lacking the C13 side chain but incorporating a 2-*m*-azide in the C2 benzoyl ring blocks cancer cell proliferation at nM concentrations.[9]

In the past few years special attention has been paid to the oxetane ring. On the basis of the inactivity of the D-seco paclitaxel **3**,[10] the oxetane ring has been considered essential for biological activity, but this hypothesis cannot be considered conclusive because **3** lacks the C4 ester group known to be crucial for activity and, compared to paclitaxel, an inverted configuration at C5. The finding that the substitution of the oxygen atom in ring D by nitrogen,[11] sulfur, or selenium atoms[12] causes a marked reduction in activity is consistent with the

† Visiting scientist from Dipartimento di Scienze Chimiche, Università di Camerino, via S. Agostino 1, 62032 Camerino (MC), Italy.

(1) Wani, M. C.; Taylor, H. L.; Wall, M. E.; Coggon, P.; McPhail, A. T. *J. Am. Chem. Soc.* **1971**, *93*, 2325−2327.
(2) Eisenhauer, E. A.; Vermorken, J. B. *Drugs* **1998**, *55*, 5−30.
(3) Holmes, F. A.; Kudelka, A. P.; Kavanagh, J. J.; Huber, M. H.; Ajani, J. A.; Valero, V. In *Taxane Anticancer Agents*; Georg, G. I., Chen, T. T., Ojima, I., Vyas, D. M., Eds.; ACS Symposium Series 583; American Chemical Society: Washington, DC, 1995; pp 31−57.
(4) *Paclitaxel in Cancer Treatment*; McGuire, W. P., Rowinsky, E. K., Eds.; Marcel Dekker: New York, 1995; Vol. 8, pp 1−349.
(5) Kingston, D. G. I. *J. Nat. Prod.* **2000**, *63*, 726−734.
(6) Landino, L. M.; Macdonald, T. L. In *The Chemistry and Pharmacology of Taxol and Its Derivatives*; Farina, V., Ed. Elsevier Science: New York, 1995; pp 301−335.
(7) Jordan, A.; Hadfield, J. A.; Lawrence, N. J.; McGown, A. T. *Med. Res. Rev.* **1998**, *18*, 259−296.
(8) Georg, G. I.; Boge, T. C.; Cheruvallath, Z. S.; Clowers, J. S.; Harriman, G. C. B.; Hepperle, M.; Park, H. In *Taxol Science and Applications*; Suffness, M., Ed.; CRC: New York, 1995; pp 317−375.
(9) He, L.; Jagtap, P. G.; Kingston, D. G. I.; Shen, H.-J.; Orr, G. A.; Horwitz, S. B. *Biochemistry* **2000**, *39*, 3972−3978.
(10) Samaranayake, G.; Magri, N. F.; Jitraugsri, C.; Kingston, D. G. I. *J. Org. Chem.* **1991**, *56*, 5114−5119.
(11) Marder-Karsenti, R.; Dubois, J.; Bricard, L.; Guénard, D.; Guéritte-Voegelein, F. *J. Org. Chem.* **1997**, *62*, 6631−6637.

10.1021/jo0015467 CCC: $20.00
Published on Web 04/18/2001

hypothesis that the C5 oxygen acts as hydrogen bond acceptor (electronic role). The D ring might also operate to rigidify the diterpenoid core, causing the side chains at C2, C4, and C13 to adopt a specific orientation for binding (conformational role).[13] Very recently[14] the role of the oxetane ring has been revised on the basis of a unified receptor model for the microtubule binding of paclitaxel and epothilone[15] and hypothesized to play both conformational and electronic roles but not to be essential for bioactivity. This proposition seems to be confirmed by the synthesis of the 5(20)deoxydocetaxel (**4**),[16] which has a cyclopropyl ring instead of the oxetane ring and lacks the C5 oxygen atom. Compound **4** is about half as

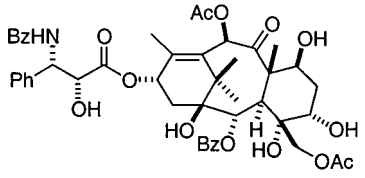

D-secopaclitaxel (**3**)

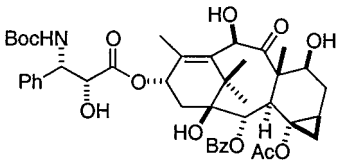

5(20)Deoxydocetaxel (**4**)

active as docetaxel on microtubules. It is reasonable that the cyclopropyl ring, as the oxetane ring, acts to rigidify the C-ring, giving the side chains a favorable orientation for binding. The absence of the C5 oxygen atom might be responsible for the slightly decreased biological activity, suggesting that the C5 oxygen could be directly involved in the interaction with microtubules. Alternatively, differential taxane solvation can also account for the activity of **4**.[14] The receptor model has also been used to predict the activity of analogues not yet synthesized[14] by employing the so-called nonpolar paclitaxel structure as a pharmacophore template for the β-tubulin/paclitaxel binding conformation. At present, the bioactive conformation is a matter of debate[15,17−19] since insufficient data have emerged to assign it unambiguously. Resolution of this problem would make an important contribution to the thinking of those who seek the next generation of paclitaxel-like drugs. Three hypothesis have emerged. On the basis of solution NMR data and molecular modeling

Scheme 1[a]

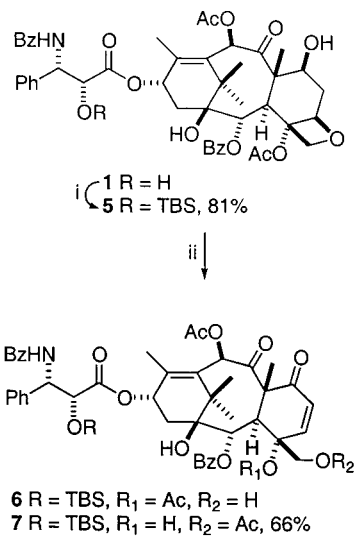

[a] (i) TBSCl, DMAP, rt, 14h; (ii) Jones reagent, acetone, rt, 30 min.

of nonataxel, Ojima and co-workers[17] proposed a pharmacophore that incorporates the hydrophobically collapsed polar conformation of paclitaxel.[19] A followup photoaffinity labeling study by the same group is rationalized in terms of the latter.[20] The same conformation in a different binding mode has been put forward by Li et al. based on fluorescence spectroscopy and REDOR NMR studies.[18] On the other hand, a pharmacophore model based on the hydrophobically collapsed nonpolar conformation of paclitaxel accounts for a wide range of taxoid and epothilone SAR.[14] More recently, a computationally refined β-tubulin−paclitaxel complex has identified an extended conformation of the drug with a C13 side chain orientation related to the nonpolar conformation, the T-conformation, as most consistent with the electron crystallographic density of the $\alpha\beta$ tubulin dimer.[21] The latter complex reinforces the notion that the oxetane ring is a rather weak hydrogen bond acceptor.

D-Secopaclitaxel Synthesis. To understand the role of the oxetane ring better and to provide probes for the evaluation of the different models for the paclitaxel binding conformation and the paclitaxel−tubulin binding site, the synthesis of D-secopaclitaxel analogues having the C4 acetate has been undertaken. Our initial target was the synthesis of D-secopaclitaxel analogues bearing an acetate group at C4 and a free hydroxy group at C20. To this end we chose the reaction reported by Magri and Kingston[22] for the oxetane ring opening, which was reported to give the 5,6-dehydro-7-oxo-5-*O*-secopaclitaxel, bearing an acetoxy group at C4 and a hydroxy group at C20. The reaction of 2′-*tert*-butyldimethysilylpaclitaxel (**5**) with the Jones reagent followed by column chromatography gave compound **7** (Scheme 1), instead of **6**, revealing a facile migration of the C4 acetate to the C20 hydroxyl, as reported for the 13-oxobaccatin III deriva-

(12) Gunatilaka, A. A. L.; Ramdayal, F. D.; Sarragiotto, M.; Kingston, D. G. I.; Sackett, D. L.; Hamel, E. *J. Org. Chem.* **1999**, *64*, 2694−2703.

(13) Boge, T. C.; Hepperle, M.; Vander Velde, D.; Gunn, C. W.; Grunewald, G. L.; Georg, G. I. *Bioorg. Med. Chem. Lett.* **1999**, *9*, 3041−3046.

(14) Wang, M.; Cornett, B.; Nettles, J.; Liotta, D. C.; Snyder, J. P. *J. Org. Chem.* **2000**, *65*, 1059−1068.

(15) Wang, M.; Xia, X.; Kim, Y.; Hwang, D.; Jansen, J. M.; Botta, M.; Liotta, D. C.; Snyder, J. P. *Org. Lett.* **1999**, *1*, 43−46.

(16) Dubois, J.; Thoret, S.; Guéritte, F.; Guénard, D. *Tetrahedron Lett.* **2000**, *41*, 3331−3334.

(17) Ojima, I.; Chakravarty, S.; Inoue, T.; Lin, S.; He, L.; Horwitz, S. B.; Kuduk, S. D.; Danishefsky, S. *Proc. Natl. Acad. Sci. U.S.A.* **1999**, *96*, 4256−4261.

(18) Li, Y.; Poliks, B.; Cegelski, L.; Poliks, M.; Gryczynski, Z.; Piszczek, G.; Jagtap, P. G.; Studelska, D. R.; Kingston, D. G. I.; Schaefer, J.; Bane, S. *Biochemistry* **2000**, *39*, 281−291.

(19) Vander Velde, D. G.; Georg, G. I.; Grunewald, G. L.; Gunn, C. W.; Mitscher, L. A. *J. Am. Chem. Soc.* **1993**, *115*, 11650−11651.

(20) Rao, S.; He, L.; Chakravarty, S.; Ojima, I.; Orr, G. A.; Horwitz, S. B. *J. Biol. Chem.* **1999**, *274*, 37990−37994.

(21) Snyder, J. P.; Nettles, J. H.; Cornett, B.; Downing, K. H.; Nogales, E. *PNAS* **2001**, in press.

(22) Magri, N. F.; Kingston, D. G. I. *J. Org. Chem.* **1986**, *51*, 797−802.

Scheme 2[a]

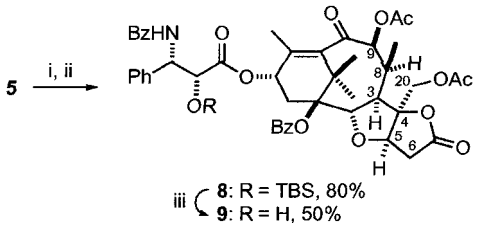

[a] (i) Jones reagent, acetone, rt, 30 min; (ii) DBU, CH_2Cl_2, rt, 1 h; (iii) HF/pyridine, pyridine, rt, 3 h.

tive.[23] The acetoxy group at C20 was detected by its HMBC correlation with H20.

A different approach to the D-seco analogue **7** has been reported and consists of the Jones oxidation of 2′-protected paclitaxel followed by treatment with DBU in CH_2Cl_2.[22] In our case this reaction gave rearranged compound **8** (Scheme 2).

The same skeletal rearrangement was reported for 13-oxobaccatin III in different conditions,[23] but in that case the C9−C10 acetoxy ketone transposition was not observed.

The ^{1}H NMR spectrum of **8** showed the presence of a proton at C8 coupled with the C3 and the C19 protons. The migration of the benzoyl group from C2 to C1 was confirmed by the upfield shift of the C2 proton from 5.57 to 5.24 ppm and the downfield shift of the C1 carbon from 73.0 to 90.6 ppm. The ^{13}C NMR of **8** lacked the C7 carbonyl signal but had a lactone carbonyl at 174.8 ppm, which showed an HMBC correlation with the C5 and the C6 protons. The presence of an acetoxy group on C20 was also confirmed in the HMBC; it additionally showed a correlation between H5 and C2. The absence of the characteristic H10 singlet and the presence of a doublet coupled with H8 indicated the acetoxy ketone transposition, confirmed by the HMBC correlation between H9 and C19. The same transposition under similar experimental conditions was previously reported for a compound having a C-seco taxoid-like skeleton.[26] It probably takes place after the skeletal rearrangement of **7**. Finally, a ROESY spectrum confirmed that H3, H5, H8, H9, and one of the H20 are on the same face of the molecule. Silyl deprotection of **8** with HF/pyridine gave compound **9**.

To prepare analogues of **7** bearing the C4 acetate group, we acetylated its C4 hydroxyl group with acetic anhydride and DMAP in toluene at 80 °C (Scheme 3).[27] The acetylation gave the desired compound **10** in acceptable yield (46%). Interestingly, during the acetylation step, new compounds **12** and **14** were formed in 13% and 2% yields, respectively. Because compound **12** gave broad NMR spectra, the structure was confirmed on the deprotected compound **13**. The most relevant spectroscopic features of **13** are the absence of the H10 signal in the ^{1}H NMR spectrum and the presence of two new non

Scheme 3[a]

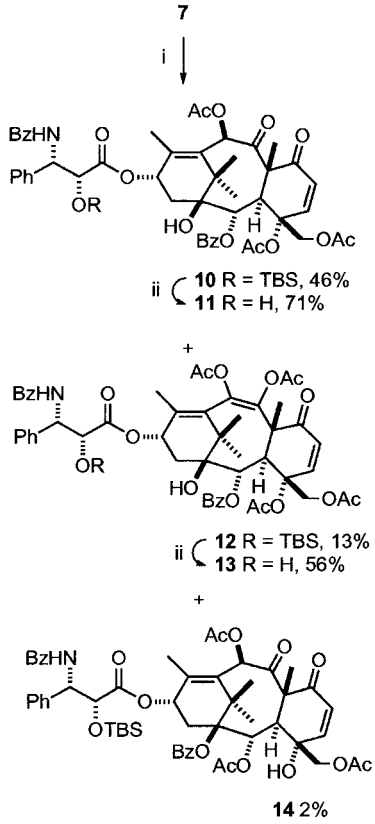

[a] (i) Ac_2O, DMAP, toluene, 80 °C, 14 h; (ii) HF/pyridine, rt, 3 h.

protonated sp^2 carbons in the ^{13}C NMR spectrum (129.57 and 136.46 ppm), one of which shows a long-range correlation with H19 in the HMBC spectrum. Compound **12** must be formed after enolization of the 9-keto group followed by acetylation of the enol. We have observed a similar reaction before, when the enol of 7,10-di-Troc-baccatin III was acylated intramolecularly to yield a 9,10 cyclic carbonate.[28] The benzoyl migration in compound **14** is indicated by the downfield shift af the C1 carbon (90.10 ppm), whereas the HMBC correlation between H2 and an acetate carbonyl confirms the presence of an acetoxy group at C2. Compound **14** is probably formed via 2-benzoyl migration and subsequent acetylation of the C2 hydroxy group. 1,2 Acyl migration of the paclitaxel 2-benzoyl group has been observed before in the reaction with CS_2.[29] Attempts to increase the yield of compound **10** by increasing the reaction time or concentration of reagents gave more complex mixtures of products.

Silyl deprotection of **10** with HF/pyridine gave compound **11**. Reduction of **10** with $NaBH_4$ in 1:1 MeOH/THF at 0 °C provided the 7α-hydroxy derivatives **15** and **17** (reduced at the Δ8 double bond) in a 3:4 ratio (Scheme 4). The stereoselectivity of the reduction is due to hydride delivery to the ketone from the more accessible β-face. Subsequent silyl deprotection afforded compounds **16** and **18**, respectively.

To invert the C7 stereochemistry to that of natural taxanes, we followed the procedure reported by Chaudhary

(23) Marder-Karsenti, R.; Dubois, J.; Chiaroni, A.; Riche, C.; Guénard, D.; Guéritte, F.; Potier, P. *Tetrahedron* **1998**, *54*, 15833−15844.
(24) Sengupta, S.; Boge, T. C.; Georg, G. I.; Himes, R. H. *Biochemistry* **1995**, *37*, 11889−11894.
(25) Ali S. M.; Hoemann, M. Z.; Aube, J.; Mitscher, L. A.; Georg, G. I.; McCall, R.; Jayasinghe, L. R. *J. Med. Chem.* **1995**, *38*, 3821−3828.
(26) Wender, P. A.; Badham, N. F.; Conway, S. P.; Floreancig, P. E.; Glass, T. E.; Houze, J. B.; Krauss, N. E.; Lee, D.; Marquess, D. G.; McGrane, P. L.; Meng, W.; Natchus, M. G.; Shuker, A. J.; Sutton, J. C.; Taylor, R. E. *J. Am. Chem. Soc.* **1997**, *119*, 2757−2758.
(27) Hoemann, M. Z.; Vander Velde, D.; Aubé, J.; Georg, G. I.; Jayasinghe, L. R. *J. Org. Chem.* **1995**, *60*, 2918−2921.
(28) Datta, A.; Aub**J**, J.; Georg, G. I.; Mitscher, L. A.; Jayasinghe, L. R. *Bioorg. Med. Chem. Lett.* **1994**, *4*, 1831−1834.
(29) Chaudhary, A. G.; Chordia, M. D.; Kingston, D. G. I. *J. Org. Chem.* **1995**, *60*, 3260−3262.

Scheme 4[a]

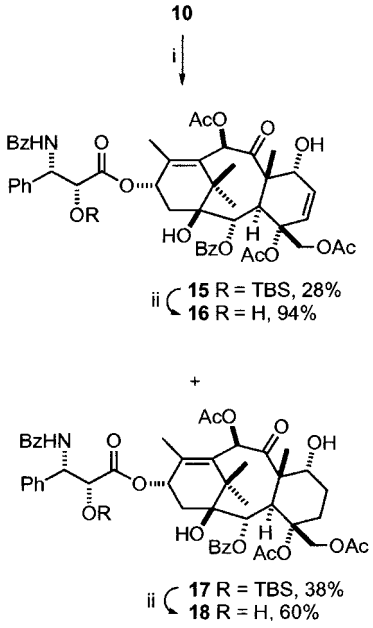

[a] (i) $NaBH_4$, MeOH/THF (1:1), 0 °C, 30 min; (ii) HF/pyridine, pyridine, rt, 3 h.

Scheme 5[a]

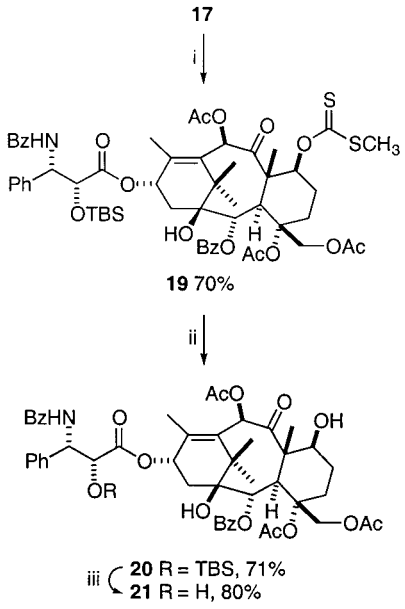

[a] (i) NaH, CS_2, CH_3I, THF, rt, 15 min; (ii) Bu_3SnH, AIBN, H_2O, toluene, 75 °C, 1 h; (iii) HF/pyridine, pyridine, rt, 3 h.

et al.[30] Treatment of compound **17** with NaH, CS_2, and MeI converted it into the *S*-methylthiocarboxy derivative **19** with the β stereochemistry at C7 (Scheme 5). Subsequent hydrolysis of **19**, achieved by treatment with Bu_3SnH and AIBN in wet toluene at 75 °C, gave compound **20** in 71% yield. Silyl deprotection yielded compound **21**.

Compounds **9**, **11**, **13**, **16**, **18**, and **21** were inactive both in cytotoxicity (MCF-7 and MCF-7/ADR) and a tubulin assembly assay.[24,25]

NMR and Conformational Analysis. We have previously published solution conformational analyses of active analogues[19,31,32] and of the inactive **3**.[13] In the latter case, conformational changes are relayed across the molecule by relaxation of the A, B, and C rings and adoption of a different preferred conformation of the C13 side chain with respect to the baccatin core.[13] Examination of the compounds reported in this paper with a saturated C ring establishes that those effects in **3** are not solely due to the opening of the D ring but also depend on the migration of the 4-acetyl out to C20. Table 1 summarizes the important *J* coupling constants in paclitaxel and three analogues. As was the case with **3**, the C ring relaxes from a flattened, strained chair to a more normal chair in **18** and **21**, as shown by the couplings involving H5, 6, and 7, but the effects on the A and B rings are much less pronounced. The origin of the A ring conformational change was investigated computationally through molecular dynamics simulations using Sybyl 6.5. The A ring conformation was characterized by the value of the torsion angle H13−C13−C14−H14β. In the crystal structure of paclitaxel, this angle has a value of 29° and 32° in the two inequivalent molecules in the unit cell.[33] In the simulation, the average value was 30°, with a bell-shaped distribution of conformers about 50° wide. This is in agreement with the approximately equal values of J_{13-14} observed in solution. In the series **11**, **16**, and **21**, removal of the D ring constraint relaxes the rigidity of the C ring and leads to a decrease in the average value of the angle in the simulations (from 30° to 18°) and an increase in the width of the distribution. In accord with the experimental finding, the two J_{13-14} values become more unequal as the 13−14β torsion approaches 0° and the 13−14α torsion moves closer to 90°. These effects are further amplified under the influence of 4-deacetylation. In simulations of 4-deacetylpaclitaxel and 4-deacetyl **21**, the average torsion angle shifted to negative values. Compound **3** displays a bimodal distribution of torsion angles, with maximum populations at small positive and small negative values. In general, the simulations indicate that the 4-acetyl moiety is actually a much more important determining factor for the A ring conformation than the D ring. This is consistent with the observation that in 10-acetyl-4-deacetyltaxotere the H13 signal is a broad doublet[34] with $J_{13-14\alpha}$ having a very small value.

D-seco compounds **11**, **16**, **18**, and **21** sustain three major orientations of the C20 side chain. As shown in Figure 1 for the saturated C ring, each arises from rotation about the axial C4/C20 bond, i.e., conformations **22a**−**22c**. In structure **22a**, the C20 C−O bond orientation is very similar to that of paclitaxel's oxetane ring, with the acetate methyl being directed away from the bulk of the molecule (Figure 2). All three conformers are internally strained as a result of 1,3-diaxial interactions. An important geometric consequence of the latter is that the C4−C20 bond is predicted by four separate force fields (MM2*, MM3*, MMFF, AMBER*)[35−37] to be partially eclipsed in each of the forms. Thus, the OC4−C20O

(30) Chaudhary, A. G.; Rimoldi, J. M.; Kingston, D. G. I. *J. Org. Chem.* **1993**, *58*, 3798−3799.

(31) Georg, G. I.; Harriman, G. C. B.; Hepperle, M.; Clowers, J. S.; Vander Velde, D. G. *J. Org. Chem.* **1996**, *61*, 2664−2676.

(32) Boge, T. C.; Himes, R. H.; Vander Velde, D. G.; Georg, G. I. *J. Med. Chem.* **1994**, *37*, 3337−3343.

(33) Mastropaolo, D.; Camerman, A.; Luo, Y.; Brayer, G. D.; Camerman, M. *Proc. Natl. Acad. Sci. U.S.A.* **1995**, *92*, 6920−6924.

(34) Datta, A.; Jayasinghe, L. R.; Georg, G. I. *J. Med. Chem.* **1994**, *37*, 4258−4260.

(35) Mohamadi, F.; Richards, N. G. J.; Guida, W. C.; Liscamp, R.; Lipton, M.; Caufield, C.; Chang, G.; Hendrickson, T.; Still, W. C. *J. Comput. Chem.* **1990**, *11*, 440−449.

Table 1. Selected ^{1}H NMR Coupling Constants[a] of Paclitaxel (1), D-Secopaclitaxel (3), 18, and 21

	$J_{2,3}$	$J_{5\alpha,6\alpha}$	$J_{5\alpha,6\beta}$	$J_{5\beta,6\alpha}$	$J_{5\beta,6\beta}$	$J_{6\alpha,7\alpha}$	$J_{6\beta,7\alpha}$	$J_{6\alpha,7\beta}$	$J_{6\beta,7\beta}$	$J_{13,14\alpha}$	$J_{13,14\beta}$
1	7.1	9.6	2.3			6.7	11.0			9.0	9.0
3	5.3			sm[b]	sm[b]	4.4	11.0			4.4	10.3
18	6.6	sm	~13.5	sm[b]	3.1			sm[b]	sm[b]	8.1	9.4
21	5.8	4.0	~13.5	sm[b]	sm[b]	4.4	11.2			7.2	9.9

[a] $CDCl_3$, 400 MHz. [b] Small but not correctly measurable.

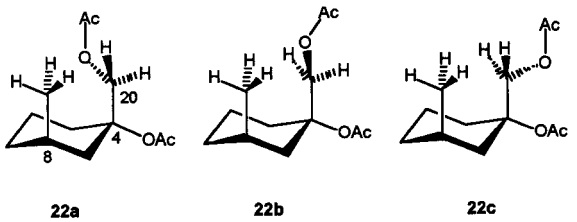

Figure 1. Rotamers around the C4−C20 bond.

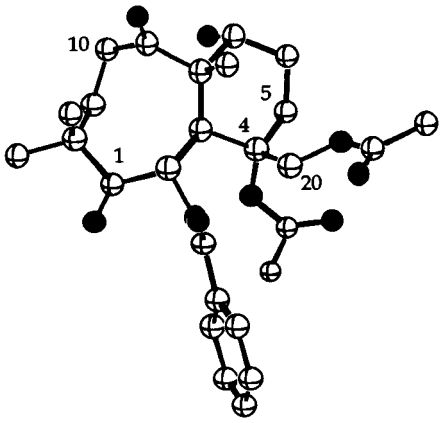

Figure 2. Partial view of compound **18b** illustrating how D-ring opening to a type **22a** conformation can mimic the oxetane ring. The C20 acetate methyl is directed away from the body of the molecule.

torsion angles are in the vicinity of 113, −95, and 30° for conformers **22a**, **22b**, and **22c**, respectively. This is not the case for the diaxial cyclohexanes that are unfused to the taxane core. For diaxial monocyclic rings, regardless of the remaining substitution pattern, the C4 and C8 diaxial groups in **22** are nicely staggered. In sharp contrast, (A)B−C ring fusion forces the axial C8 methyl in the direction of C4. As a result, there is a pronounced gearing effect between the axial centers and the C2 benzoyl group that causes a less than ideal local orientation of the C4−C20 bond. As described above, conformational changes are relayed between rings A and D in taxol. These are relaxed to some extent when ring D is severed. At the same time, relaxation is not complete. The bicyclic A−B architecture still appears to exert a forceful influence on the C ring (e.g., the 19-Me tilt angle) as measured by molecular mechanics.

To examine the conformational profile of the C ring in the context of the full C13 side chain bearing structure, we performed a NAMFIS analysis[38−40] on compound **18**. NMR coupling constants and ROESY cross-peak volumes taken in DMSO-d_6 were thus combined with 5126 conformations obtained from conformational searches with four separate force fields using an aqueous continuum model (see Experimental Section). Unlike previous NAMFIS analyses,[38,39] the present one must be taken as more qualitative than quantitative, since the cross-peaks were characterized only as strong, medium, and weak. To the latter, we have assigned separation values of 2.7, 3.5, and 4.0 Å, respectively. Using the corresponding 29 ROE-derived distances and six coupling constants (Table 1), the 5126 conformer collection was deconvoluted to a set of seven conformations with estimated populations ranging from 6 to 46% and with a sum of square differences SSD = 44.[38] Of the seven, three are in the **22a** family and four in the **22b** family. No representatives of **22c** are compatible with the NMR data, although the conformational data set contains many such representatives. Of the three most populated forms **18a**, **18b**, and **18c** (46, 13, and 11%, respectively), the first and third incorporate the features of **22b**, the second, **22a**. Not unexpectedly, **18a** is very similar to the polar conformation deduced from NMR studies in DMSO-d_6/D_2O showing hydrophobic collapse between the C2 and C3′ phenyl groups.[19] The 169° HC2′−C3′H dihedral angle corresponds to $J_{H2'H3'}$ = 10.6 Hz.[42] Of the six remaining conformations, three also adopt a variation of the polar conformer leading to an estimated total of 71% polar character in the conformational profile of **18**. Evidence has been presented both for and against the "hydrophobic collapse" as the bioactive conformation of taxanes. However, from both active[32] compounds that do not adopt this conformation, and inactive compounds that do (this work), it is clear that the population of this conformation in solution does not correlate with bioactivity.

Interestingly, the second and third most populated structures **18b** and **18c** are extended conformers. In this respect, the D-seco analogue **18** resembles paclitaxel in both nonpolar[39] and polar[40] solvents. That is, while the dominant conformation represents the family character with respect to hydrophobic collapse, a not insignificant fraction of the perceived conformers are extended forms. More importantly, the latter structures bear a close resemblance to an emerging model regarding the binding conformation of paclitaxel at the β-tubulin binding site, namely, the T conformation.[21] Figure 3 illustrates the nonpolar, polar, and T conformations. Superposition of the A and B rings in **18b** and T-paclitaxel results in a remarkably similar placement of the four terminal hydrophobes emanating from C2, C4, and C3′. A key difference between paclitaxel and the inactives **18** and

(36) Still, W. C.; Tempczyk, A.; Hawley, R. C.; Hendrickson, T. *J. Am. Chem. Soc.* **1990**, *112*, 6127−6129.
(37) Cf. http://www.schrodinger.com/macromodel2.html.
(38) Nevins, N.; Cicero, D. O.; Snyder, J. P. *J. Org. Chem.* **1999**, *65*, 3979−3986.
(39) Snyder, J. P.; Nevins, N. N.; Cicero, D. O.; Jansen, J. *J. Am. Chem. Soc.* **2000**, *122*, 724−725.
(40) Nevins, N. N.; Cicero, D. O.; Jansen, J.; Jiminez-Barbero, J.; Snyder, J. P. (unpublished results).
(41) Four of the conformations sustain gauche interactions for the HC2′−C3′H torsional angle; two, 175−180°. As a result, the final weighted conformational average yields $J_{H2'H3'}$ = 7.9 Hz as the fit to the experimental value of 6.4 Hz.
(42) Nogales, E.; Wolf, S. G.; Downing, K. H. *Nature* **1998**, *391*, 199−202.

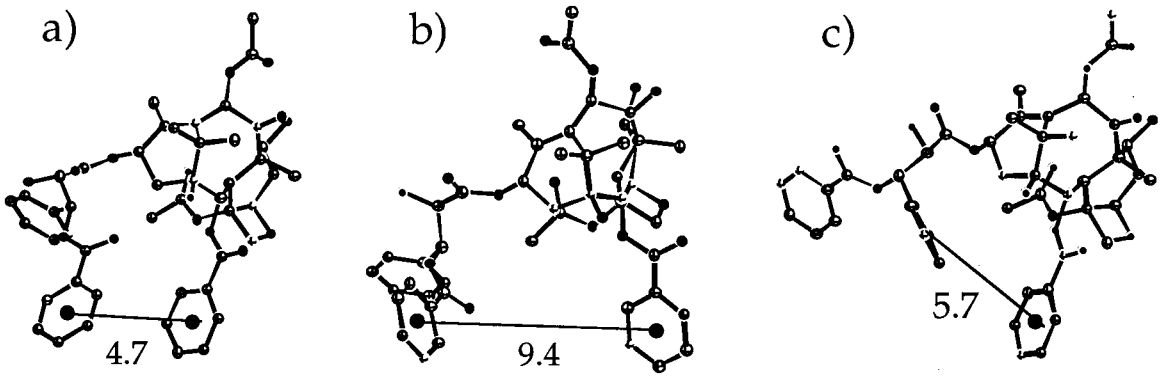

Figure 3. Graphical representations of the three conformations of paclitaxel. The depicted distances (**C**) are between the centroids of the phenyl rings at C2 and C3′. Only the closest of the two rings at C3′ are labeled: (a) nonpolar, (b) T-paclitaxel, (c) polar conformation.

Table 2. Prediction of the Binding Affinities of D-Seco Paclitaxel Analogues by the Second-Generation Paclitaxel−Epothilone Minireceptor Model

	K_{pred} (M)	K_{pred}/K_{TX}	ΔG_{solv} (kcal/mol)
paclitaxel	2.9e-5	1	−13.2
11	2.3e-3	79	−23.0
16	1.5e-3	52	−20.6
18	1.0e-4	3.5	−15.7
21	2.5e-5	0.9	−16.13

21 is the steric bulk at C20 in the latter. Given the availability of the T-rotational form to the D-seco analogues, it implies that the disrupted D-ring and the orientation of the pendant substitutents are responsible for the lack of activity (see below).

Minireceptor Predictions. Prior to synthesis, we predicted the **22a** analogues of D-seco analogues **11** and **16** to bind β-tubulin only weakly relative to paclitaxel but **18** and **21** to be similar to the drug in their binding affinities (Table 2). Unfortunately, in light of the biological data described above, the second-generation model[15] overpredicts binding of the compounds by a factor of 10−60.

The basis for the lack of agreement between experiment and prediction lies in the constitution of the minireceptor in the vicinity of the oxetane ring. In this model, a conservative set of β-tubulin protein residues taken from photoaffinity labeling experiments was employed. In particular, we selected an Arg to form a strong hydrogen bond with the oxetane oxygen but did not supplement this region of the receptor with other side chains. With the availability of the electron crystallography structure of $\alpha\beta$ tubulin[42] and complementary modeling studies,[14] it has become clear that the H-bond to the oxetane is rather weak and supplied by the neutral residue Thr instead of cationic Arg. For oxetane ring replacements such as thietane and cyclopropane, the arginine model is sufficient to account for bioactivity.[14] However, the present synthetic and biological results add another critical requirement to the receptor model. Namely, additional residues are necessary to accommodate local ligand−protein steric effects around the opened oxetane ring. In an evolving third-generation minireceptor construct, a threonine and two leucines were positioned in close contact with the C4−C5 four-membered ring in accord with the complementary locations of Thr276, Leu217, and Leu275 in the tubulin protein.[43] When conformations corresponding to **22a** are docked into this receptor cavity, the terminal CH_3 group of the acetate at C20 in the D-seco compounds is sterically blocked by Leu217. Likewise, when the less stable conformations **22b** are docked into the site, an equally unproductive interaction arises from close contact between the C20 acetate methyl and Leu275. These modeling observations are fully consistent with the results of the conformational analysis described in the previous section. Not surprisingly, the enhanced minireceptor model predicts that **11**, **16**, **18**, and **21** all bind to β-tubulin with an affinity at least 100 times less than that of paclitaxel.

Conclusion

In summary, four novel D-seco paclitaxel analogues bearing acetate groups at C4 and C20 were prepared. All compounds were inactive in cytotoxicity and tubulin assembly assays. Conformational analysis and dynamics simulations strongly suggest that the tetracyclic taxane core is capable of a hierarchy of inter-ring transmission effects. On one hand, removal of the D ring has a decisive influence on the conformations of the A and C rings. Flattened in the four-ring core, the latter assumes a more relaxed shape in the D-seco analogues. Nonetheless, the intact AB pair still appears to exert a gearing effect on the axial substitutents of the C ring. Surprisingly, as judged by J_{13-14} changes and dynamics simulation, the largest determining factor for the A ring conformation is the presence of the 4-acetyl moiety. As to prediction of biological activity, the present results illuminate an important weakness in our second-generation minireceptor model and a strategy for correcting it. Clearly, bulky groups at C5 and C20 will impair the activity of paclitaxel analogues even though the molecule can adopt what we believe to be the bioactive form (T-paclitaxel) at the β-tubulin binding site.

Experimental Section

General Methods. Cytotoxicity and tubulin binding were carried out according to established literature protocols[24,25] except that the MCF-7 breast cancer cell line was used in the cytotoxicity assays. Commercially available reagents and solvents were used without further purification. CH_2Cl_2 was dried by distillation from CaH_2, and THF by distillation from Na−benzophenone. Flash column chromatography was carried out with silica gel as the stationary phase. Jones reagent was prepared as follows: CrO_3 (1.67 g, 0.017 mmol) was dissolved

(43) Wang, M.; Snyder, J. P. (unpublished results).

in water (2.5 mL). The solution was cooled at 0 °C and concentrated H_2SO_4 (1.44 mL) was added. Then water was added up to 7 mL.

20-Acetyl-2′-*O*-(*tert*-butyldimethylsilyl)-4-deacetyl-5,6-dehydro-7-oxo-5-*O*-secopaclitaxel (7). Compound **5**[44] (785 mg, 0.81 mmol) was dissolved in acetone (15 mL, freshly distilled from $KMnO_4$), and freshly prepared Jones reagent (1.6 mL) was added. After stirring for 30 min at room temperature (TLC monitoring), 2-propanol was added as the solution turned green. Then brine was added and the solution extracted with EtOAc (4 × 15 mL). The combined extract was dried over Na_2SO_4, filtered, and evaporated under vacuum. After flash column chromatography on silica gel (9:1 to 4:1 hexane/EtOAc), 520 mg of compound **7** (0.54 mmol, 66%) was collected as an amorphous solid. ^{1}H NMR (400 MHz, $CDCl_3$): δ −0.30 (s, 3H), −0.11 (s, 3H), 0.81 (s, 9H), 1.06 (s, 3H), 1.20 (s, 3H), 1.54 (s, 3H), 1.73 (s, 3H), 1.92 (s, 3H), 2.22 (s, 3H), 2.41 (dd, J = 15.7, 10.6, 1H), 2.94 (dd, J = 15.7, 4.4 Hz, 1H), 4.13 (d, J = 12.0, 1H), 4.15 (d, J = 6.0, 1H), 4.32 (d, J = 12.0, 1H), 4.45 (bs, 1H), 5.57 (d, J = 6.0, 1H), 5.86 (bd, J = 9.8, 1H), 6.03 (d, J = 10.3, 1H), 6.05 (bd, J = 8.3, 1H), 6.38 (s, 1H), 7.02 (d, J = 10.3, 1H), 7.18 (t, J = 7.7), 7.26−7.53 (m, 9H), 7.57 (bt, J = 7.2, 1H), 7.81 (bd, J = 7.7, 2H), 8.13 (bd, J = 7.9, 2H). ^{13}C NMR (100 MHz, $CDCl_3$): δ −5.53, −5.16, 16.33, 18.66, 19.07, 20.63, 21.34, 25.95, 27.82, 30.10, 36.24, 43.00, 54.40, 55.54, 63.71, 67.32, 72.16, 73.03, 74.75, 75.90, 77.92, 123.46, 126.92, 127.42, 128.24, 128.76, 128.92, 129.27, 129.34, 130.92, 132.27, 133.89, 134.80, 135.37, 140.08, 140.19, 155.75, 167.47, 168.05, 169.64, 170.62, 170.65, 198.53, 199.73. MS (ES$^+$) m/z 988 (M + Na)$^+$, 966 (M + H)$^+$, 567, 549, 507, 400.

Compound 8. To a CH_2Cl_2 (5 mL) solution of compound **7** (150 mg, 0.16 mmol) was added DBU (509 mg, 0.5 mL, 3.3 mmol), and the reaction mixture was stirred at room temperature for 1 h. Then CH_2Cl_2 and HCl (1 N) were added. The organic layer was washed with saturated $NaHCO_3$ and brine and dried over Na_2SO_4. After filtration, evaporation of the solvent and flash column chromatography (3:2 hexane/EtOAc), 120 mg of compound **8** (0.124 mmol, 80%) was collected as an amorphous solid: ^{1}H NMR (400 MHz, $CDCl_3$) δ −0.34 (s, 3H), −0.08 (s, 3H), 0.79 (s, 9H), 1.24 (s, 3H), 1.26 (d, J = 7.1, 3H), 1.31 (s, 3H), 2.06 (bs, 6H), 2.24 (s, 3H), 2.45 (dd, J = 16.5, 6.1, 1H), 2.55 (d, J = 18.6, 1H), 2.77 (m, 2H), 2.91 (m, 1H), 3.25 (dd, J = 16.5, 9.9, 1H), 4.16 (d, J = 11.9, 1H), 4.66 (d, J = 1.8, 1H), 5.06 (d, J = 11.9, 1H), 5.20 (bd, J = 6.1, 1H), 5.26 (d, J = 8.6, 1H), 5.40 (d, J = 6.7, 1H), 5.91 (dd, J = 9.3, 1.7, 1H), 5.98 (bt, J = 7.7, 1H), 7.12 (d, J = 9.4, 1H), 7.30 (m, 1H), 7.40 (m, 8H), 7.52 (m, 2H), 7.84 (m, 4H); ^{13}C NMR (100 MHz, $CDCl_3$) δ −5.64, −4.99, 12.71, 18.18, 18.61, 21.00, 21.07, 22.54, 25.91, 27.36, 35.08, 37.63, 42.63, 50.52, 56.07, 67.21, 71.10, 76.03, 79.36, 82.05, 82.92, 90.62, 96.17, 127.15, 127.51, 128.20, 128.72, 128.93, 129.17, 129.99, 132.03, 132.08, 133.06, 134.89, 138.90, 139.46, 141.69, 165.26, 167.53, 170.57, 170.67, 170.85, 174.76, 199.60; MS (FAB$^+$) m/z 965, 845, 445, 400, 354, 210, 177, 154.

Compound 9. To an ice cooled solution of compound **8** (50 mg, 0.052 mmol) in dry pyridine (3 mL) was added HF·pyridine (25 drops), and the mixture was stirred at room temperature for 3 h (TLC check, 3:2 hexane/EtOAc). The solution was then neutralized with saturated $NaHCO_3$, acidified with 3 N HCl, and extracted with CH_2Cl_2 (3 × 10 mL). The organic layer was washed with brine and then dried over Na_2SO_4, filtered, and evaporated. After flash column chromatography (7:3 hexane/EtOAc), 22 mg of compound **9** (0.026 mmol, 50%) was collected as a colorless powder: mp 142−144 °C; ^{1}H NMR (400 MHz, $CDCl_3$) δ 1.23 (s, 3H), 1.23 (d, J = 7.0, 3H), 1.30 (s, 3H), 2.00 (s, 3H), 2.02 (s, 3H), 2.21 (s, 3H), 2.53 (d, J = 18.8, 1H), 2.59 (dd, J = 16.7, 6.1, 1H), 2.73 (dd, J = 18.7, 5.8 1H), 2.76 (d, J = 8.5, 1H), 2.88 (m, 1H), 3.35 (dd, J = 16.7, 9.8, 1H), 3.37 (bs, 1H), 4.28 (d, J = 11.8, 1H), 4.79 (bt, J = 2.0, 1H), 4.92 (d, J = 11.8, 1H), 5.13 (d, J = 8.3, 1H), 5.21 (bd, J = 5.8, 1H), 5.37 (d, J = 6.7, 1H), 5.93 (dd, J = 9.7, 1.8, 1H), 5.98 (m, 1H), 6.98 (d, J = 9.7, 1H), 7.32 (bt, J = 7.4, 1H), 7.36−7.44 (m, 7H), 7.49 (bt, J = 7.6, 2H), 7.54 (bt, J = 7.3, 1H), 7.79 (bd, J = 7.7, 2H), 7.90 (bd, J = 7.9, 2H); ^{13}C NMR (100 MHz, $CDCl_3$) δ 12.72, 18.21, 20.98, 21.07, 22.32, 27.56, 34.05, 35.08, 37.78, 42.61, 50.40, 54.69, 67.00, 72.22, 73.93, 79.57, 82.65, 82.85, 90.17, 96.25, 127.44, 127.55, 128.51, 128.78, 129.15, 129.25, 130.00, 132.01, 132.25, 133.17, 134.52, 138.73, 139.69, 141.28, 165.36, 167.56, 170.60, 170.74, 172.56, 174.77, 199.43; IR ($CHCl_3$) 3470, 1810, 1760, 1730, 1675, 1540, 1380, 1250 cm^{-1}; FAB HRMS m/z calcd for (M + H)$^+$ $C_{47}H_{50}NO_{14}$ 852.3231, found 852.3261; $[\alpha]^{20}_D$ 124 (c 1.00, $CHCl_3$).

Acetylation of compound 7. Compound **7** (200 mg, 0.21 mmol) was dissolved in toluene (10 mL); then DMAP (122 mg, 1 mmol) and Ac_2O (790 μL, 857 mg, 8.4 mmol) were added. The reaction mixture was stirred under argon at 80 °C for 17 h (the solution turned brown, TLC check showed some starting material but the reaction was worked up to avoid decomposition); then the solvent was concentrated under vacuum and the residue was dissolved in CH_2Cl_2 and washed with saturated $NaHCO_3$. The aqueous solution was extracted with CH_2Cl_2 (3 × 15 mL), and the combined organic layers were washed with brine and then dried over Na_2SO_4, filtered, and evaporated. After flash column chromatography on silica gel (4:1 to 7:3 hexane/EtOAc), 80 mg of compound **10** (0.079 mmol, 38%), 28 mg of **12** (0.026 mmol, 13%), and 4 mg of **14** (0.004 mmol, 2%) were collected.

Compound 10. Amorphous solid: ^{1}H NMR (400 MHz, $CDCl_3$) δ −0.35 (s, 3H), −0.06 (s, 3H), 0.76 (s, 9H), 1.18 (s, 3H), 1.20 (s, 3H), 1.63 (s, 3H), 1.85 (s, 3H), 1.89 (s, 3H), 2.18 (m, 1H, 14), 2.21 (s, 3H), 2.48 (s, 3H), 2.79 (dd, J = 15.3, 8.6 Hz, 1H), 4.27 (d, J = 13.1, 1H), 4.33 (d, J = 7.0, 1H), 4.52 (d, J = 13.1, 1H), 4.67 (d, J = 1.9, 1H), 5.65 (d, J = 7.0, 1H), 5.80 (dd, J = 9.2, 1.9, 1H), 6.07 (d, J = 10.6, 1H), 6.27 (bt, J = 8.7, 1H), 6.36 (s, 1H), 7.08 (d, J = 9.2, 1H), 7.18 (d, J = 10.6, 1H), 7.26−7.62 (m, 11H), 7.77 (bd, J = 8.1, 2H), 8.10 (bd, J = 7.8, 2H); ^{13}C NMR (100 MHz, $CDCl_3$) δ −5.48, -4.81, 15.00, 17.91, 18.52, 20.87, 21.27, 21.32, 23.30, 25.89 (x3), 26.52, 30.11, 35.89, 43.53, 51.30, 55.96, 63.79, 68.16, 70.99, 74.55, 75.72, 76.85, 79.32, 82.97, 124.77, 126.70, 127.40, 128.30, 129.13, 129.23, 129.30, 129.80, 130.48, 132.26, 132.42, 134.31, 134.57, 138.72, 141.58, 149.18, 167.31, 167.57, 169.54, 169.87, 171.65, 196.99, 199.48; IR ($CHCl_3$) 3465, 2960, 1760, 1690, 1520, 1240 cm^{-1}; MS (FAB$^+$) m/z 1008 (M + H)$^+$, 948, 549, 489, 400, 354.

Compound 12. Amorphous solid: ^{1}H NMR (400 MHz, $CDCl_3$, 50 °C) δ −0.34 (s, 3H), −0.03 (s, 3H), 0.79 (s, 9H), 1.23 (s, 3H), 1.44 (s, 3H), 1.68 (s, 3H), 1.84 (s, 3H), 1.86 (s, 3H), 2.06 (s, 3H), 2.18 (s, 3H), 2.27 (m, 1H, 14), 2.50 (s, 3H), 2.90 (dd, J = 15.0, 7.6 Hz, 1H), 3.94 (d, J = 5.3, 1H), 4.14 (d, J = 12.5, 1H), 4.60 (d, J = 12.5, 1H), 4.64 (bs, 1H), 5.79 (bd, J = 9.1, 1H), 5.98 (d, J = 5.3, 1H), 6.07 (d, J = 10.6, 1H), 6.21 (bt, J = 8.9, 1H), 7.08 (d, J = 9.1, 1H), 7.24 (d, J = 10.6, 1H), 7.26−7.61 (m, 11H), 7.79 (bd, J = 7.8, 2H), 8.06 (bd, J = 7.8, 2H); ^{13}C NMR (125 MHz, $CDCl_3$) δ −5.85, −5.16, 16.48, 18.10, 20.24, 20.44, 20.51, 20.77, 21.37, 23.92, 25.50, 35.53, 43.28, 49.64, 55.14, 55.81, 66.30, 70.71, 74.67, 75.56, 78.93, 83.39, 126.21, 126.31, 126.71, 126.96, 127.28, 127.75, 128.64, 128.83, 129.66, 129.85, 130.10, 130.59, 134.50, 136.71, 138.84, 139.06, 143.90, 146.48, 166.34, 166.91, 167.01, 168.01, 169.15, 169.37, 171.00, 194.96; MS (FAB+) m/z 1051 (M + H)$^+$, 991, 400, 354.

Compound 14. Amorphous solid: ^{1}H NMR (400 MHz, $CDCl_3$) δ −0.27 (s, 3H), −0.11 (s, 3H), 0.83 (s, 9H), 1.12 (s, 3H), 1.39 (s, 3H), 1.52 (s, 3H), 1.89 (s, 3H), 1.94 (s, 3H), 1.99 (s, 3H), 2.22 (s, 3H), 2.96 (dd, J = 16.4, 4.5 Hz, 1H), 3.78 (dd, J = 16.4, 10.2 Hz, 1H), 4.12 (d, J = 11.9, 1H), 4.18 (d, J = 6.1, 1H), 4.39 (d, J = 11.9, 1H), 4.49 (d, J = 1.6, 1H), 5.28 (s, 1H), 5.65 (d, J = 6.1, 1H), 5.95 (m, 1H), 6.03 (bd, J = 8.5, 1H), 6.06 (d, J = 10.4, 1H), 6.33 (s, 1H), 7.17 (d, J = 10.6, 1H), 7.25−7.67 (m, 12H), 7.67 (bd, J = 8.3, 2H), 7.83 (bd, J = 7.8, 2H); ^{13}C NMR (100 MHz, $CDCl_3$) δ −5.46, −5.16, 16.17, 18.64, 18.68, 20.79, 20.98, 21.34, 21.56, 25.95, 28.81, 44.60, 54.45, 55.62, 63.62, 67.46, 71.49, 72.90, 73.83, 75.63, 77.03, 90.09, 123.42, 127.32, 127.80, 128.16, 128.79, 128.82, 128.92, 129.80, 131.32, 131.92, 133.22, 133.28, 135.14, 140.01, 141.19, 156.93, 164.76, 168.01, 169.53, 170.98, 171.13, 171.33, 197.98, 199.29; MS (FAB+) m/z 1008 (M + H)$^+$, 950, 852, 826, 705.

(44) Magri, N. F.; Kingston, D. G. I. *J. Nat. Prod.* **1988**, *51*, 298−306.

Compound 11. To an ice cooled solution of compound **10** (30 mg, 0.030 mmol) in dry pyridine (3 mL) was added HF·pyridine (20 drops), and the mixture was stirred at room temperature for 3 h (TLC check, 3:2 hexane/EtOAc). The solution was then neutralized with saturated $NaHCO_3$, acidified with 3 N HCl, and extracted with CH_2Cl_2 (3 × 10 mL). The organic layer washed with brine and then dried over Na_2SO_4, filtered, and evaporated. After flash column chromatography (3:2 hexane/EtOAc), 19 mg of compound **11** (0.021 mmol, 71%) was collected as a colorless powder: mp 150−152 °C; ^{1}H NMR (400 MHz, $CDCl_3$) δ 1.15 (s, 3H), 1.19 (s, 3H), 1.60 (s, 3H), 1.61 (s, 3H), 1.89 (s, 3H), 2.20 (s, 3H), 2.31 (s, 3H), 2.40 (dd, J = 15.5, 9.7, 1H), 2.50 (dd, J = 15.5, 7.6, 1H), 3.96 (d, J = 4.2, 1H), 4.25 (d, J = 13.0, 1H), 4.28 (d, J = 6.9, 1H), 4.51 (d, J = 13.0, 1H), 4.78 (dd, J = 4.2, 2.6, 1H), 5.62 (d, J = 6.9, 1H), 5.80 (dd, J = 9.1, 2.6, 1H), 6.02 (d, J = 10.6, 1H), 6.11 (bt, J = 8.5, 1H), 6.30 (s, 1H), 6.97 (d, J = 10.6, 1H), 7.19 (d, J = 9.1, 1H), 7.28−7.54 (m, 10H), 7.61 (bt, J = 7.7, 1H), 7.77 (bd, J = 7.7, 2H), 8.07 (bd, J = 7.7, 2H); ^{13}C NMR (100 MHz, $CDCl_3$) δ 14.95, 17.95, 20.64, 20.87, 21.25, 22.95, 26.71, 36.04, 43.35, 51.01, 55.15, 63.84, 68.27, 71.80, 74.06, 74.29, 76.90, 79.12, 83.42, 124.81, 127.42, 127.46, 128.66, 129.16, 129.24, 129.29, 129.68, 130.40, 132.40, 132.92, 134.11, 134.39, 138.45, 140.79, 149.14, 167.11, 167.47, 169.44, 169.92, 170.40, 172.04, 196.75, 199.27; IR ($CHCl_3$) 3490, 1750, 1670, 1540, 1230 cm^{-1}; FAB HRMS m/z calcd for $(M + H)^+$ $C_{49}H_{52}NO_{15}$ 894.3337, found 894.3362; $[\alpha]^{20}_D$ −58 (c 0.70, $CHCl_3$).

Compound 13. To an ice cooled solution of compound **12** (60 mg, 0.057 mmol) in dry pyridine (3 mL) was added HF·pyridine (25 drops), and the mixture was stirred at room temperature for 3 h (TLC check, 3:2 hexane/EtOAc). The solution was then neutralized with saturated $NaHCO_3$, acidified with 3 N HCl, and extracted with CH_2Cl_2 (3 × 10 mL). The organic layer was washed with brine and then dried over Na_2SO_4, filtered, and evaporated. After flash column chromatography (3:2 hexane/EtOAc), 30 mg of compound **13** (0.032 mmol, 56%) was collected as a colorless powder: mp 148−150 °C; ^{1}H NMR (400 MHz, $CDCl_3$) δ 1.22 (s, 3H), 1.43 (s, 3H), 1.63 (bs, 3H), 1.66 (s, 3H), 1.88 (s, 3H), 2.08 (s, 3H), 2.20 (s, 3H), 2.38 (s, 3H), 2.43 (dd, J = 15.2, 10.0, 1H), 2.58 (dd, J = 15.2, 7.0, 1H), 3.92 (bs, 1H), 4.04 (d, J = 4.0 Hz), 4.10 (bd, J = 12.6, 1H), 4.59 (d, J = 12.6, 1H), 4.80 (dd, J = 4.0, 2.6, 1H), 5.79 (bd, J = 9.4, 1H), 5.95 (d, J = 5.4, 1H), 6.02 (d, J = 10.7, 1H), 6.11 (bt, J = 8.5, 1H), 7.04 (d, J = 10.7, 1H), 7.15 (d, J = 9.4, 1H), 7.30−7.55 (m, 10H), 7.62 (bt, J = 7.3, 1H), 7.79 (bd, J = 7.8, 2H), 8.06 (bd, J = 7.8, 2H); ^{13}C NMR (100 MHz, $CDCl_3$) δ 16.43, 18.90, 20.36, 20.52, 20.88, 21.12, 22,66, 23.95, 35.80, 43.13, 49.50, 55.01, 55.11, 66.50, 71.51, 73.95, 74.55, 78.95, 83.68, 125.92, 127.00, 127.07, 128.13, 128.71, 128.81, 128.87, 129.57, 129.97, 130.84, 131.83, 133.73, 134.04, 136.46, 138.46, 138.90, 143.03, 146.48, 166.26, 166.91, 166.98, 168.05, 169.24, 169.82, 171.73, 194.70; IR ($CHCl_3$) 3480, 1750, 1700, 1530, 1225 cm^{-1}; FAB HRMS m/z calcd for $(M + H)^+$ $C_{51}H_{54}NO_{16}$ 936.3443, found 936.3397; $[\alpha]^{20}_D$ 30 (c 0.90, $CHCl_3$).

Reduction of Compound 10. To an ice cooled solution of compound **10** (100 mg, 0.1 mmol) in 1:1 MeOH/THF (20 mL) was added $NaBH_4$ (19 mg, 0.5 mmol). The reaction mixture was stirred at 0 °C for 25 min (TLC check, 3:2 hexane/EtOAc); then 3 N HCl was added, the solvent was concentrated under vacuum, and the residue was diluted with CH_2Cl_2 and washed with water. The aqueous solution was extracted with CH_2Cl_2 (3 × 15 mL), and the organic layer was washed with brine and then dried over Na_2SO_4. After filtration, evaporation of the solvent, and flash column chromatography (7:3 hexane/EtOAc), 28 mg of compound **15** (0.028 mmol, 28%) and 38 mg of compound **17** (0.038 mmol, 38%) were collected.

Compound 15. Amorphous solid: ^{1}H NMR (400 MHz, $CDCl_3$) δ −0.37 (s, 3H), −0.08 (s, 3H), 0.74 (s, 9H), 1.13 (s, 3H), 1.16 (s, 3H), 1.34 (s, 3H), 1.69 (s, 3H), 1.94 (s, 3H), 2.13 (dd, J = 15.5, 8.8, 1H), 2.18 (s, 3H), 2.45 (s, 3H), 2.51 (dd, J = 15.5, 9.3 Hz, 1H), 3.61 (dd, J = 10.1, 5.7 1H), 4.20 (d, J = 12.5, 1H), 4.27 (d, J = 12.5, 1H), 4.50 (d, J = 8.6, 1H), 4.66 (d, J = 1.9, 1H), 5.68 (d, J = 8.6, 1H), 5.69 (d, J = 10.1, 1H), 5.86 (dd, J = 9.1, 1.9, 1H), 6.01 (dd, J = 10.1, 5.7 1H), 6.27 (bt, J = 9.1, 1H), 6.99 (s, 1H), 7.06 (d, J = 9.1, 1H), 7.25−7.56 (m, 11H), 7.74 (bd, J = 8.1, 1H), 8.18 (bd, J = 8.5, 1H); ^{13}C NMR (100 MHz, $CDCl_3$) δ −6.07, −5.33, 14.11, 15.47, 16.78, 20.23, 20.91, 23.23, 25.44, 25.91, 36.59, 42.18, 43.69, 55.49, 58.58, 68.52, 70.35, 72.89, 75.54, 75.99, 78.49, 80.09, 82.31, 126.30, 127.01, 127.78, 127.81, 128.71, 128.72, 128.80, 130.09, 130.31, 130.96, 131.28, 131.74, 133.37, 134.20, 138.45, 140.21, 166.80, 167.77, 169.65, 170.10, 170.93, 171.41, 205.96; MS (FAB$^+$) m/z 1010 $(M + H)^+$, 1009, 950, 768, 491, 400, 354, 210, 177.

Compound 17. Amorphous solid: ^{1}H NMR (400 MHz, $CDCl_3$) δ −0.33 (s, 3H), −0.07 (s, 3H), 0.78 (s, 9H), 1.11 (s, 3H), 1.19 (s, 3H), 1.48 (s, 3H), 1.58 (m, 1H), 1.91 (s, 3H), 1.95 (s, 3H), 1.95 (m, 1H), 2.01 (m, 1H), 2.15 (m, 1H), 2.19 (s, 3H), 2.41 (s, 3H), 2.89 (m, 1H), 3.23 (dd, J = 15.0, 8.9 Hz, 1H), 3.58 (bs, 1H), 3.76 (d, J = 6.6, 1H), 4.16 (d, J = 13.9, 1H), 4.44 (d, J = 13.9, 1H), 4.66 (d, J = 1.9, 1H), 5.71 (d, J = 6.6, 1H), 5.76 (dd, J = 9.0, 1.9, 1H), 6.31 (bt, J = 8.9, 1H), 6.89 (s, 1H), 7.12 (d, J = 9.0, 1H), 7.25−7.58 (m, 11H), 7.79 (bd, J = 7.7, 1H), 8.03 (bd, J = 7.8, 1H); ^{13}C NMR (100 MHz, $CDCl_3$) δ −5.84, −5.30, 15.04, 17.63, 18.15, 20.65, 20.91, 21.42, 23.08, 25.51, 26.27, 27.19, 35.48, 42.70, 47.67, 55.72, 59.26, 67.05, 71.34, 74.97, 75.41, 76.20, 79.12, 79.68, 85.46, 126.32, 126.42, 127.00, 127.15, 127.84, 128.65, 128.79, 129.89, 131.77, 132.77, 133.59, 134.26, 138.51, 140.49, 166.76, 167.61, 168.97, 169.61, 170.30, 171.38, 206.66; MS (FAB$^+$) m/z 1012 $(M + H)^+$, 952, 493, 400, 354, 210, 177.

Compound 16. To an ice cooled solution of compound **15** (30 mg, 0.030 mmol) in dry pyridine (3 mL) was added HF·pyridine (20 drops), and the mixture was stirred at room temperature for 3 h (TLC check, 3:2 hexane/EtOAc). The solution was then neutralized with saturated $NaHCO_3$, acidified with 3 N HCl, and extracted with CH_2Cl_2 (3 × 10 mL). The organic layer was washed with brine and then dried over Na_2SO_4, filtered, and evaporated. After flash column chromatography (3:2 hexane/EtOAc), 25 mg of compound **16** (0.028 mmol, 94%) was collected as a colorless powder: mp 153−155 °C; ^{1}H NMR (400 MHz, $CDCl_3$) δ 1.13 (bs, 6H), 1.33 (s, 3H), 1.72 (bs, 3H), 1.75 (s, 3H), 2.18 (s, 3H), 2.31 (s, 3H), 2.33 (m, 2H), 2.96 (d, J = 9.8 Hz), 3.60 (dd, J = 9.8, 5.7 1H), 3.69 (d, J = 3.4 Hz), 4.15 (d, J = 12.6, 1H), 4.33 (d, J = 12.6, 1H), 4.47 (d, J = 8.4, 1H), 4.80 (bt, J = 3.4, 1H), 5.62 (d, J = 10.2, 1H), 5.68 (d, J = 8.4, 1H), 5.89 (bd, J = 9.7, 1H), 5.99 (dd, J = 10.2, 5.7 1H), 6.14 (bt, J = 8.1, 1H), 6.94 (s, 1H), 7.15 (d, J = 9.7, 1H), 7.20−7.60 (m, 11H), 7.76 (bd, J = 7.8, 2H), 8.16 (bd, J = 7.6); ^{13}C NMR (100 MHz, $CDCl_3$) δ 16.00, 17.09, 20.74, 21.10, 21.33, 23.38, 26.69, 36.89, 42.47, 44.17, 54.72, 59.05, 69.01, 71.99, 73.09, 74.04, 76.13, 79.04, 80.34, 83.35, 125.92, 127.31, 127.47, 128.48, 129.09, 129.17, 129.25, 130.42, 130.63, 131.00, 132.28, 132.45, 133.94, 134.23, 138.63, 139.74, 166.96, 168.15, 169.96, 170.41, 171.97, 172.21, 205.95; IR ($CHCl_3$) 3460, 1750, 1675, 1530, 1240 cm^{-1}; MS (FAB+) m/z 896 $(M + H)^+$, 836, 778, 654, 491; HRMS (FAB+) m/z calcd for $(M^+ - OAc)$ $C_{47}H_{50}NO_{13}$ 836.3281, found 836.3275; $[\alpha]^{20}_D$ −24 (c 0.80, $CHCl_3$).

Compound 18. To an ice cooled solution of compound **17** (30 mg, 0.030 mmol) in dry pyridine (3 mL) was added HF·pyridine (20 drops), and the mixture was stirred at room temperature for 3 h (TLC check, 3:2 hexane/EtOAc). The solution was then neutralized with saturated $NaHCO_3$, acidified with 3 N HCl, and extracted with CH_2Cl_2 (3 × 10 mL). The organic layer washed with brine and then dried over Na_2SO_4, filtered, and evaporated. After flash column chromatography (3:2 hexane/EtOAc), 16 mg of compound **18** (0.018 mmol, 60%) was collected as a colorless powder: mp 160−162 °C; ^{1}H NMR (400 MHz, $CDCl_3$) δ 1.11 (s, 3H), 1.18 (s, 3H), 1.46 (s, 3H), 1.60 (m, 1H), 1.77 (s, 3H), 1.89 (s, 3H), 1.99 (m, 1H), 2.19 (s, 3H), 2.23 (m, 1H), 2.26 (s, 3H), 2.34 (dd, J = 15.2, 9.4, 1H), 2.69 (bd, J = 13.3, 1H), 3.01 (dd, J = 15.3, 8.1 Hz, 1H), 3.56 (bs, 1H), 3.63 (d, J = 5.0, 1H), 3.85 (d, J = 6.6, 1H), 4.16 (d, J = 13.6, 1H), 4.40 (d, J = 13.6, 1H), 4.78 (dd, J = 5.0, 2.5, 1H), 5.70 (d, J = 6.6, 1H), 5.79 (dd, J = 9.0, 2.5, 1H), 6.17 (bt, J = 8.1, 1H), 6.85 (s, 1H), 7.09 (d, J = 9.0, 1H), 7.28−7.60 (m, 11H), 7.79 (bd, J = 8.0, 2H), 8.03 (bd, J = 8.0, 2H); ^{13}C NMR (100 MHz, $CDCl_3$) δ 15.43, 18.10, 21.06, 21.31, 21.37, 23.22, 26.22, 26.26, 27.61, 35.90, 42.95, 47.74, 55.41, 59.84, 67.29, 72.79, 73.89, 75.20, 76.44, 79.42, 80.13, 86.30, 127.42, 127.49, 128.66,

129.11, 129.13, 129.34, 130.29 (x2), 132.34, 133.52, 134.04, 134.20, 138.54, 140.22, 167.24, 168.01, 169.70, 170.11, 170.73, 172.78, 206.98; IR ($CHCl_3$) 3480, 1750, 1680, 1535, 1260 cm^{-1}; FAB HRMS *m/z* calcd for $(M + H)^+$ $C_{49}H_{56}NO_{15}$ 898.3650, found 898.3641; $[\alpha]^{20}_D$ −49 (*c* 0.70, $CHCl_3$).

Compound 19. To a suspension of NaH (2.3 mg, 0.095 mmol, 4 g of 60% dispersion) in dry THF (0.5 mL)was added compound **17** (53 mg, 0.052 mmol), dissolved in dry THF (0.5 mL). The reaction mixture was stirred at room temperature for 5 min, and CS_2 (50 μL) and MeI (50 μL) were added. After 15 min at room temperature, EtOAc (5 mL) and water (5 mL) were added. The mixture was extracted with EtOAc (3 × 10 mL) and the organic layer dried over Na_2SO_4 and evaporated. After flash column chromatography (4:1 hexane/EtOAc), 40 mg of compound **19** (0.036 mmol, 70%) was collected as an amorphous solid: ^{1}H NMR (400 MHz, $CDCl_3$) δ −0.29 (s, 3H), −0.02 (s, 3H), 0.81 (s, 9H), 1.21 (s, 3H), 1.25 (s, 3H), 1.56 (m, 1H), 1.57 (s, 3H), 1.80 (m, 1H), 1.98 (s, 3H), 2.07 (bs, 3H), 2.16 (d, J = 3.3 Hz, 1H), 2.28 (m, 2H), 2.42 (s, 3H), 2.47 (s, 3H), 3.36 (dd, J = 15.2, 7.9 Hz, 1H), 3.43 (bd, J = 13.6 Hz, 1H), 3.53 (d, J = 5.5 Hz, 1H), 4.12 (d, J = 13.9, 1H), 4.43 (d, J = 13.9, 1H), 4.67 (d, J = 1.8, 1H), 5.62 (d, J = 5.5, 1H), 5.74 (bd, J = 9.1, 1H), 5.87 (dd, J = 11.4, 4.6 Hz, 1H), 6.33 (bt, J = 8.7, 1H), 6.44 (s, 1H), 7.13 (d, J = 9.1, 1H), 7.27−7.61 (m, 11H), 7.80 (bd, J = 7.5, 2H), 7.99 (bd, J = 7.9, 2H); ^{13}C NMR (100 MHz, $CDCl_3$) δ −5.32, −4.76, 12.78, 16.13, 18.55, 18.83, 20.57, 21.04, 21.18, 23.30, 25.93, 26.03, 32.84, 35.31, 44.16, 54.71, 56.14, 58.77, 67.18, 71.96, 75.03, 75.60, 75.71, 78.34, 82.59, 84.49, 126.63, 127.40, 128.40, 129.14, 129.19, 129.28, 129.84, 130.18, 132.29, 133.77, 134.25, 134.59, 138.63, 140.70, 167.43 (x2), 169.26, 169.38, 169.74, 171.89, 201.56, 215.39; MS (FAB^+) *m/z* 1102, 1042, 643, 583, 535, 493, 479, 400, 354.

Compound 20. A solution of Bu_3SnH (200 μL), AIBN (3 mg), and H_2O (40 μL) in toluene (1 mL) was heated at 75 °C under an argon atmosphere. A solution of compound **19** (35 mg, 0.032 mmol) in dry toluene (1 mL) was added, and the reaction mixture was stirred at 75 °C (TLC check, 7:3 hexane/EtOAc). After 1 h EtOAc was added and the solvent evaporated under vacuum. The mixture was purified as follows: the column was first washed with hexane to eliminate the excess of Bu_3SnH and then eluted with 4:1 to 3:7 hexane/EtOAc, collecting 23 mg of compound **20** (0.023 mmol, 71%) as an amorphous solid: ^{1}H NMR (400 MHz, $CDCl_3$) δ −0.27 (s, 3H), −0.04 (s, 3H), 0.82 (s, 9H), 1.17 (s, 3H), 1.25 (s, 3H), 1.39 (s, 3H), 1.48 (m, 1H), 1.80 (m, 1H), 1.93 (m, 1H), 1.95 (s, 3H), 1.99 (bs, 3H), 2.14 (d, J = 3.3 Hz, 1H), 2.24 (s, 3H), 2.25 (dd, J = 15.1, 9.7 Hz, 1H), 2.42 (s, 3H), 3.28 (dd, J = 15.1, 8.3 Hz, 1H), 3.31 (bd, J = 13.5 Hz, 1H), 3.43 (d, J = 5.9 Hz, 1H), 3.88 (m, 1H), 4.12 (d, J = 13.8, 1H), 4.40 (d, J = 13.8, 1H), 4.67 (d, J = 1.9, 1H), 5.64 (d, J = 5.9, 1H), 5.75 (bd, J = 9.1, 1H), 6.33 (bt, J = 8.8, 1H), 6.47 (s, 1H), 7.13 (d, J = 9.1, 1H), 7.30−7.61 (m, 11H), 7.80 (bd, J = 7.6, 2H), 8.01 (bd, J = 8.0, 2H); ^{13}C NMR (100 MHz, $CDCl_3$) δ −5.31, −4.85, 10.93, 15.87, 18.57, 21.01, 21.27, 23.43, 25.93, 26.80, 26.96, 32.96, 35.32, 43.93, 52.94, 56.09, 61.58, 67.07, 72.07, 74.80, 75.41, 75.73, 75.97, 79.07, 84.79, 126.71, 127.39, 128.39, 129.14, 129.17, 129.25, 130.01, 130.21, 132.29, 133.87, 134.16, 134.57, 138.67, 141.85, 167.29, 167.65, 169.22, 169.86, 171.37, 171.98, 204.02; MS (FAB^+) *m/z* 1011, 953, 553, 493, 451, 400, 354.

Compound 21. To an ice cooled solution of compound **20** (34 mg, 0.034 mmol) in dry pyridine (3 mL) was added HF·pyridine (20 drops), and the mixture was stirred at room temperature for 3 h (TLC check, 1:1 hexane/EtOAc). The solution was then neutralized with saturated $NaHCO_3$, acidified with 3 N HCl, and extracted with CH_2Cl_2 (3 × 10 mL). The organic layer was washed with brine and then dried over Na_2SO_4, filtered, and evaporated. After flash column chromatography (2:3 hexane/EtOAc), 24 mg of compound **21** (0.027 mmol, 80%) was collected as a colorless powder: mp 159−161 °C; ^{1}H NMR (400 MHz, $CDCl_3$) δ 1.15 (s, 3H), 1.23 (s, 3H), 1.35 (s, 3H), 1.54 (m, 1H), 1.76 (m, 1H), 1.79 (s, 3H), 1.89 (m, 1H), 1.93 (s, 3H), 2.10 (d, J = 3.5 Hz, 1H), 2.23 (s, 3H), 2.24 (m, 1H, 5), 2.43 (dd, J = 15.4, 9.9, 1H), 3.08 (dd, J = 15.4, 7.2 Hz, 1H), 3.16 (m, 1H), 3.46 (d, J = 5.8 Hz, 1H), 3.56 (d, J = 5.9, 1H), 3.86 (m, 1H), 4.08 (d, J = 13.7, 1H), 4.36 (d, J = 13.7, 1H), 4.79 (dd, J = 6.0, 2.7, 1H), 5.59 (d, J = 5.8, 1H), 5.75 (dd, J = 8.9, 2.7, 1H), 6.18 (bt, J = 8.2, 1H), 6.43 (s, 1H), 7.07 (d, J = 8.9, 1H), 7.33−7.49 (m, 9H), 7.54 (bt, J = 7.4, 1H), 7.59 (bt, J = 7.4, 1H), 7.80 (bd, J = 7.8, 2H), 7.98 (bd, J = 8.1, 2H); ^{13}C NMR (100 MHz, $CDCl_3$) δ 10.97, 15.85, 20.88, 21.01, 21.31, 23.05, 26.87, 27.24, 32.55, 35.37, 43.70, 52.84, 55.88, 61.65, 67.03, 72.96, 73.94, 74.72, 75.50, 75.72, 78.90, 84.94, 127.48 (×2), 128.85, 129.12, 129.21, 129.45, 129.96, 130.17, 132.52, 133.97, 134.18, 134.24, 138.18, 141.32, 167.53, 167.64, 169.39, 169.94, 171.39, 172.83, 203.86; IR ($CHCl_3$) 3434, 1729, 1654, 1518, 1245 cm^{-1}; FAB HRMS *m/z* calcd for $(M + H)^+$ $C_{49}H_{56}NO_{15}$ 898.3650, found 898.3619; $[\alpha]^{20}_D$ −98 (*c* 0.90, $CHCl_3$).

Computational Procedures. Structure **18** was subjected to Monte Carlo conformational searches with the AMBER*, MM2*, MM3*, and MMFF force fields and the GB/SA/H_2O continuum model in MacroModel6.5[35−37] for a total of 35 000 steps. The global minima were located 13, 5, 2, and 10 times, respectively. The combined set of 5126 optimized conformers was treated to a NAMFIS[38] conformer deconvolution analysis by fitting 29 rOe's and six J couplings. The rOe cross-peaks were classified as weak, medium, and strong. Since NAMFIS requires explicit distances as input, the latter were assigned average values of 4.0, 3.5, and 2.7 Å, respectively. The experimental J values were converted to dihedral angles with the modified Karplus equation due to Haasnoot, Leeuw, and Altona.[45] The NAMFIS fitting procedure provided seven conformations with predicted populations ranging from 6 to 46%, i.e., 46, 13, 11, 9, 8, 7, and 6%, with a sum of square differences (SSD) of 44. The corresponding O−C4−C20O optimized torsional angles are −105, 116, −82, −89, 112, −87, and 113°, respectively. All structures were visualized on SGI O2 workstations and further manipulated in MacroModel; for example, for evaluation of the effect of B−C ring fusion on the axial−axial interaction between C8-Me and C4-CH_2OAc and for the nature of the hydrophobic collapse between C2 and C3′ phenyl rings.

Molecular dynamics simulations to investigate the effect of D-ring opening and 4-deacetylation were performed in Sybyl 6.5 using the Sybyl force field and Gasteiger-Hückel partial atomic charges.

Acknowledgment. We acknowledge the National Cancer Institute (1R01 CA-82801) and the Drug Discovery Program, Higuchi Biosciences Center, for financial support and DABUR INDIA Ltd. for a generous gift of paclitaxel. The authors thank Rebecca Marquez for performing the biological assays. L.B. is grateful to Consiglio Nazionale delle Ricerche, Italy, for a Mobilità di breve durata fellowship.

Supporting Information Available: ^{1}H and ^{13}C spectra of compounds **11**, **16**, **18**, and **21**. This material is available free of charge via the Internet at http://pubs.acs.org.

JO0015467

(45) Haasnoot, C. G. G.; De Leeuw, F. A. A. M.; Altona, C. *Tetrahedron* **1980**, *36*, 2783−2792.